ChemComm

COMMUNICATION

View Article Online
View Journal | View Issue

Adsorption and reaction of sub-monolayer films of an ionic liquid on Cu(111)†

Cite this: *Chem. Commun.*, 2014, 50, 8601

Received 29th April 2014,
Accepted 12th June 2014

DOI: 10.1039/c4cc03203a

www.rsc.org/chemcomm

Benedikt Uhl,‡[ab] Florian Buchner,‡[ab] Stephan Gabler,[ab] Maral Bozorgchenani[ab] and R. Jürgen Behm*[ab]

The reactive interaction of the ionic liquid 1-butyl-1-methylpyrrolidinium bis(trifluoromethylsulfonyl)imide [BMP][TFSA] with Cu(111) was investigated by scanning tunnelling microscopy (STM) and X-ray photoelectron spectroscopy (XPS) under ultrahigh vacuum (UHV) conditions. Decomposition between 300 K and 350 K is manifested by changes in the surface structure monitored with STM. XPS reveals that mainly the [TFSA] anion is decomposed.

Ionic liquids (ILs), which are defined as molten salts with a melting point below 100 °C,[1] have attracted rapidly increasing attention due to their outstanding physicochemical properties such as high ionic conductivity and electrochemical stability, very low vapour pressure, or low flammability.[1–3] Furthermore, these properties can be systematically tuned by varying the combination of anion–cation pairs. Among other applications, ILs were identified to be particularly suitable for application in the area of electrochemical energy storage, as a solvent in lithium ion and lithium air batteries.[4–6] For a systematic optimization of the ILs for these applications, a detailed understanding of the processes at the IL|solid interface on a fundamental level, at the molecular scale, is essential, which is a precondition for understanding the processes leading to the formation of the solid-electrolyte interphase in Li ion batteries. This led to a number of studies on the interaction between ILs and solid electrode surfaces, both *in situ*, under electrochemical conditions,[7–9] and *ex situ*, under ultrahigh vacuum (UHV) conditions.[10,11] Molecular scale information on the adsorption behaviour directly at the IL|metal interface, in the monolayer regime, however, is scarce and is just starting to emerge.

Therefore we have recently started to systematically investigate the interaction between representative ILs, which are suitable for battery applications, and selected electrode materials. In a first step, we focussed on idealized materials, specifically noble metal surfaces, and idealized conditions, at the solid|vacuum interface under UHV conditions. In these studies we concentrated on aspects of structure formation, the chemical state of the molecules at the interface, and the interactions between metal and adsorbed ILs. Following previous reports on the interaction of the anion–cation pair 1-butyl-1-methylpyrrolidinium bis (trifluoromethylsulfonyl)imide [BMP][TFSA] with the rather inert Ag(111) and Au(111) surfaces,[12–15] in the present communication we make a considerable step forward towards the ultimate goal of understanding the processes leading to the formation of the solid-IL interphase (SEI), exploring the interaction of [BMP][TFSA] with the more reactive Cu(111) surface. We here present first results on the interaction of submonolayer amounts of [BMP][TFSA] with Cu(111), employing scanning tunnelling microscopy (STM) and X-ray photoelectron spectroscopy (XPS) for structural and chemical characterization, respectively. Considering the higher reactivity of Cu(111) compared to Ag(111) and Au(111), we will compare our findings with results obtained for the interaction of the same IL with Ag(111) and Au(111), where this had been demonstrated to adsorb intact, without decomposition, up to at least 420 K.[12–15]

In the present work, we are particularly interested in the thermal stability and decomposition of the adsorbed IL in the temperature range between liquid nitrogen temperature and around room temperature (300–350 K). Following our approach for [BMP][TFSA] adsorption on Ag(111) and Au(111), we first performed STM measurements on a sub-monolayer [BMP][TFSA] film covered Cu(111) surface, where both IL deposition and STM imaging were performed at around room temperature.

In large scale STM images (Fig. 1a and b) we find noisy terraces with no obvious structure. This resembles previous findings for [BMP][TFSA] adsorption on Au(111) and Ag(111) (see Fig. 2a for comparison), where STM imaging at room temperature also resulted in structureless, noisy images.[12–15] The noisy appearance was explained by mobile adsorbates rapidly diffusing over the

[a] *Helmholtz Institute Ulm Electrochemical Energy Storage, Albert-Einstein-Allee 11, D-89081 Ulm, Germany. E-mail: juergen.behm@uni-ulm.de; Fax: +49 (0)731/50-25452; Tel: +49 (0)731/50-25451*

[b] *Ulm University, Institute of Surface Chemistry and Catalysis, Albert-Einstein-Allee 47, D-89081 Ulm, Germany. E-mail: juergen.behm@uni-ulm.de; Fax: +49 (0)731/50-25452; Tel: +49 (0)731/50-25451*

† Electronic supplementary information (ESI) available: Experimental part. See DOI: 10.1039/c4cc03203a

‡ These authors contributed equally.

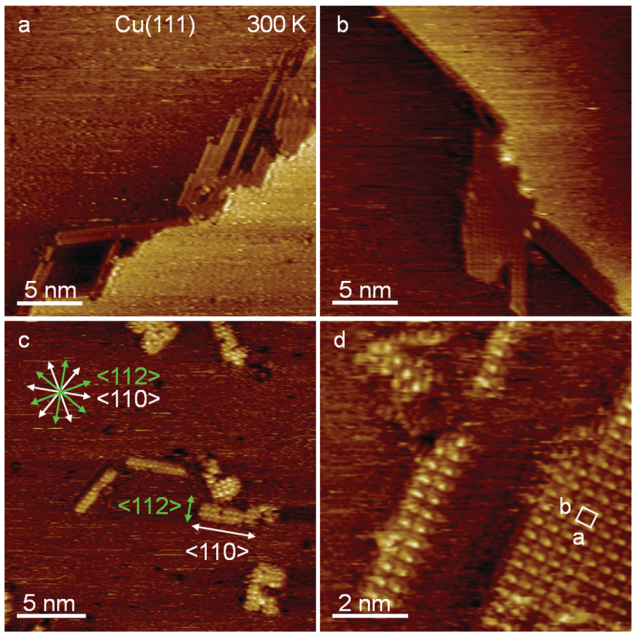

Fig. 1 STM images recorded after vapor deposition of [BMP][TFSA] on Cu(111) at room temperature reveal a modification of the steps (imaging temperature 300 K). In (a) and (b) it is demonstrated that the steps are in large parts modified by ordered structures. (c) These commensurate structures also appear at the terraces, exhibiting distinct azimuthal orientation along the main axes of the underlying copper atomic lattice. In the magnified STM image in (d) the unit cell is highlighted.

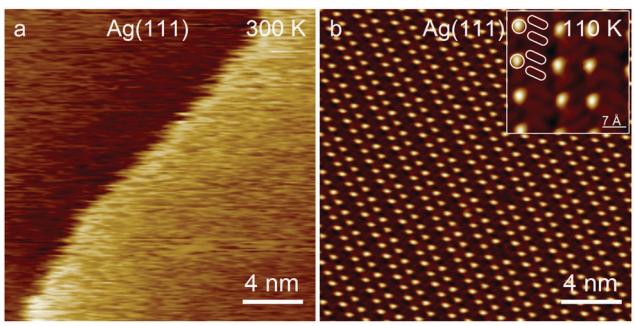

Fig. 2 STM images after (a) vapour deposition of [BMP][TFSA] on Ag(111) at room temperature (imaged at r.t.) (b) after cool down to liquid nitrogen temperature. The noisy appearance at room temperature is indicative for a 2D gas/liquid adlayer. Upon cool down a highly ordered 2D solid phase is formed. The insert in Fig. 2b resolves dots and pairs of longish protrusions, which are assigned to the alkyl chains of the cation pointing towards vacuum and the two CF_3 groups in the anion, respectively (details are found in ref. 14).

surface. Furthermore, and different from the findings for the latter adsorption systems, the step edges changed their shape from straight or slightly curved on the bare, adsorbate free Cu(111) surface into steps with clear preferential orientations which differ by angles of $\pm 120^\circ$, indicative of step faceting. Upon closer inspection we also find small and long shaped islands with ordered structure, either attached to the steps (see Fig. 1a and b) or located on the terraces as demonstrated in Fig. 1c. Time sequences of STM images verify that these islands are highly stable over time, pointing to a rather high barrier for diffusion on the Cu(111) surface. The high stability and the pronounced anisotropic shape of the islands indicate strong and highly anisotropic interactions between neighbouring adspecies, with a much stronger interaction along the long island direction than orthogonal to it. Comparison with atomic resolution images of the Cu(111) lattice reveals that the islands are strictly aligned along the main directions of the underlying copper lattice, with the long side oriented along the close-packed $<110>$ directions and the short side along the $<112>$ directions. The dimensions of the unit cell are $|a| = 0.47 \pm 0.02$ nm and $|b| = 0.52 \pm 0.2$ nm and $\alpha = 90 \pm 2^\circ$ (Fig. 1d), the resulting commensurate overlayer can be described by a $\begin{vmatrix} 2 & 1 \\ 0 & 2 \end{vmatrix}$ superstructure, using standard matrix notation. The structure of the islands is very different from that of the [BMP][TFSA] adlayer formed on Ag(111) or Au(111) upon cooling down to liquid nitrogen temperature (see Fig. 2b for comparison). Most important, the size of the unit cell is too small for a [BMP][TFSA] adlayer, considering the size of the adsorbed ion pairs (*ca.* 0.9 nm diameter per adsorbed ion[14]). Therefore the STM images provide first evidence for a decomposition of the adsorbed [BMP][TFSA] film under these conditions, where the islands are composed of a rather small adsorbed fragment of the decomposition process. In that case, the other remaining fragments of the decomposition process are either desorbed or are present as highly mobile adspecies, contributing to the noisy appearance of the remaining terrace areas. For larger exposures, the islands with their square structure grow in size.

In the next step, a submonolayer of [BMP][TFSA] was prepared on Cu(111) by vapour deposition on the sample held at around 200 K and subsequent cool down to $\sim$100 K (note that similar structures were observed upon deposition at $\sim$100 K and subsequent imaging at that temperature (see ESI†)). In the large scale STM image in Fig. 3a (300 nm $\times$ 150 nm) the surface is covered by a 0.4 ML [BMP][TFSA] adlayer, where the adsorbed species are condensed into small island structures which are homogeneously distributed over the terraces (1 monolayer (ML) corresponds to the number of adsorbed ions in direct contact with the surface at saturation). Also in this case the steps are decorated; however, they are not altered as described above upon vapour deposition at 300 K. The magnified STM image inserted in Fig. 3a resolves that the islands exhibit branched shapes and consist of a disordered pattern of protrusions. Hence, despite using a higher sample temperature for preparing the adlayer (200 K), ordering still seems to be kinetically limited. Different from adsorption on Ag(111),[14] it was not possible to resolve and identify individual anions and cations, and also the typical structural element observed upon adsorption on Ag(111) or Au(111), with one circular protrusion for the cation and two parallel elliptic protrusions for the anion, could not be resolved.

Beside the structural information gained from STM imaging, the chemical state of the adlayer was probed by XPS measurements. Representative C1s and S2p core level spectra recorded after deposition on the sample held at 80 K, are depicted in Fig. 3b and c. A molecular stick presentation of [BMP][TFSA] is placed above the spectra. In the C1s region (Fig. 3b), the peak referred to as C_{alkyl} (285.0 eV) can be associated with five carbon atoms, three in the butyl group and two in the 5-membered ring,

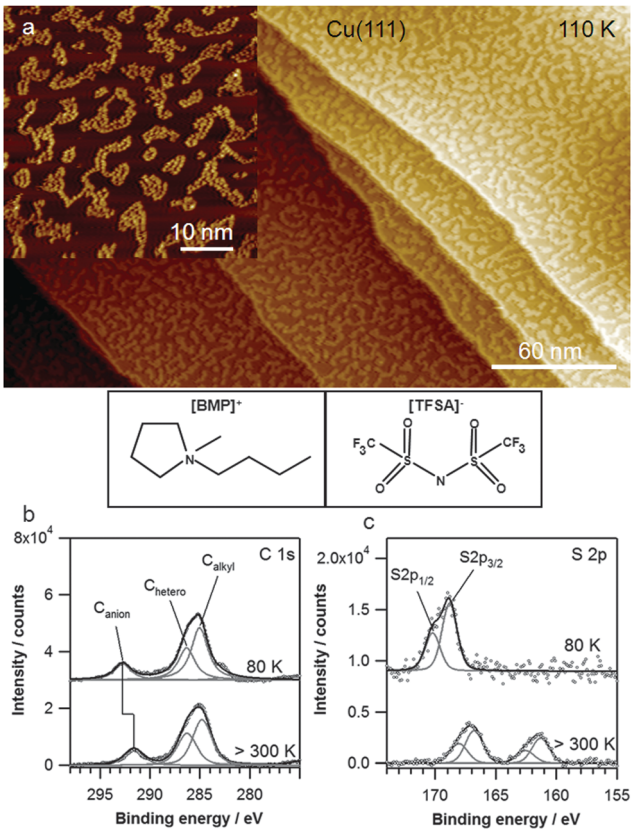

Fig. 3 (a) STM image recorded after vapour deposition of [BMP][TFSA] on Cu(111) held at 200 K and subsequent cool down to 110 K, showing islands with arbitrary shape. (b) and (c) XP spectra recorded upon annealing an adlayer prepared by vapour deposition on Cu(111) held at 80 K to 300 K, revealing chemical changes in the C1s and S2p regions of the anion upon annealing to around 300 K.

where each group has a similar carbon environment. In a similar way, the peak referred to as C_{hetero} (286.2 eV) is related to the four carbon atoms which are next to the nitrogen atom of the ring. The C_{anion} (292.7 eV) peak is finally assigned to the two carbon atoms in the anion. The nominal intensity ratio of these peak areas is 5 : 4 : 2, experimentally we found a ratio of 5.0 : 4.0 : 1.8 (normalized to C_{alkyl}). This agrees well with the stoichiometry of the molecules, in the limits of the experimental accuracy. The S2p core level signal shows the $S2p_{1/2}$ and $S2p_{3/2}$ doublet at 170.3 eV and 168.9 eV, respectively, caused by the sulphur atom in the SO_2 group of the anion. The F1s and O1s regions reveal single peaks at 688.7 and 532.6 eV, respectively, which also originate from the [TFSA] anion. Also their intensities agree rather well with the nominal values expected for intact IL adsorbates. The N1s region unfortunately overlaps with a background feature, it is therefore not shown. Overall, the XP data indicate that intact [BMP][TFSA] species are adsorbed on Cu(111) at 80 K which is supported also by the absence of the ordered square structure in STM images as shown in Fig. 1. Similar structures as in Fig. 3a were observed also upon IL deposition at temperatures below 200 K and subsequent STM imaging at ~100 K.

To elucidate temperature-induced changes, we also performed XPS measurements at around room temperature. Distinct differences in the spectra compared to those recorded after deposition at 80 K indicate that under these conditions the adlayer has changed considerably (Fig. 3b and c). The C1s spectrum in Fig. 3b shows that the peaks related to C_{alkyl} and C_{hetero} persist and are essentially unaffected, while the peak due to C_{anion} shifts by 1.1 eV to lower binding energy (291.6 eV); the total peak area is nearly constant. Also the F1s peak shifts by 0.5 eV to lower BEs (688.2 eV), with a constant peak area. The constant intensity and the BE shifts of the signals in the F1s and C1s regions indicate changes of the atomic environment of these atoms, while their total amount remains constant, *i.e.*, it is not affected by desorption. In contrast, the O1s intensity decreases by roughly 60%, indicative of a loss of oxygen containing species due to desorption. Marked changes occur in particular in the S2p region (Fig. 3c), where two new doublets evolve, which must reflect the formation of two new adspecies, while the intensities of the previous peaks decay to zero. The doublet with BEs of 162.5 and 161.3 eV is ascribed to adsorbed atomic sulphur (S_{ad}) or to Cu_xS. Earlier STM[16] and low energy electron diffraction (LEED)[17] studies on the chemisorption of sulphur on Cu(111) had shown that deposition of S, by exposure to H_2S, caused a distinct restructuring of the steps, which closely resembled our findings (see Fig. 1). Furthermore, they resolved a number of different stable surface structures, depending on the H_2S exposure. These structures differ from the square structure detected in the present study (Fig. 1), but this may result from the presence of coadsorbed species. Therefore we assume that the stable adsorbate structure formed at room temperature (Fig. 1) is composed of S_{ad} or Cu_xS. The doublet at 168.0 and 166.8 eV probably stems from adsorbed SO_x. The total intensity in the S2p region remains constant. Together with the constant intensities of the C1s, S2p, F1s peaks and the decrease of the O1s intensity this points to a decomposition of the adsorbed [TFSA] anion into mainly Cu_xS (or S_{ad}), SO_x, and probably other fluoro and carbon containing species ($CF_{3,ad}$).

In summary, the interaction of [BMP][TFSA] with the more reactive Cu(111), as compared to Ag(111) or Au(111), can be characterized by the following features:

(1) Upon deposition at low temperatures (80–200 K) [BMP][TFSA] adsorbs intact on Cu(111), forming islands with branched, quasi-dendritic shapes. This reflects attractive interactions between adsorbed species. Different from the noble metal surfaces, no long-range ordered structures are formed, which we attribute to a too low mobility of the adspecies at these temperatures.

(2) Vapour deposition of [BMP][TFSA] on Cu(111) at room temperature causes a decomposition of the [BMP][TFSA], specifically of the adsorbed [TFSA] anions, while the cations remain intact. Interaction of the rather mobile Cu(111) surface with the decomposition products, most likely with adsorbed S, causes a restructuring of the steps (step faceting), together with the formation of a stable adsorbate phase with a square lattice. Other decomposition products on the surface might be SO_x and fluoro/carbon containing adspecies ($CF_{3,ad}$), which are too mobile for the visualization by STM at room temperature.

(3) Heating the surface to ~300 K after low temperature deposition of [BMP][TFSA] results in dissolution of the islands observed at low temperatures, in combination with anion decomposition, step restructuring and formation of an S_{ad} phase

as experienced upon adsorption at room temperature (see STM image ESI†).

Overall, these findings provide first molecular scale information on the decomposition of an IL upon interaction with a reactive surface such as Cu(111), which can be considered as a further step toward understanding the processes leading to the formation of the solid-electrolyte interphase (SEI) in a Li ion battery.

This work was financially supported by the ''Fonds der chemischen Industrie (FCI)''.

Notes and references

1 T. Welton, *Chem. Rev.*, 1999, **99**, 2071.
2 P. Wasserscheid and W. Keim, *Angew. Chem., Int. Ed.*, 2000, **39**, 3772.
3 N. V. Plechkova and K. R. Seddon, *Chem. Soc. Rev.*, 2008, **37**, 123.
4 M. Armand and J.-M. Tarascon, *Nature*, 2008, **451**, 652.
5 M. Armand, F. Endres, D. R. MacFarlane, H. Ohno and B. Scrosati, *Nat. Mater.*, 2009, **8**, 621.
6 G. Girishkumar, B. McCloskey, A. C. Luntz, S. Swanson and W. Wilcke, *J. Phys. Chem. Lett.*, 2010, **1**, 2193.
7 F. Endres, O. Höfft, N. Borisenko, L. H. Gasparotto, A. Prowald, R. Al-Salman, T. Carstens, R. Atkin, A. Bund and S. Z. El Abedin, *Phys. Chem. Chem. Phys.*, 2010, **12**, 1724.
8 R. Atkin, N. Borisenko, M. Drüschler, S. Z. El Abedin, F. Endres, R. Hayes, B. Huber and B. Roling, *Phys. Chem. Chem. Phys.*, 2011, **13**, 6849.
9 M. Drüschler, N. Borisenko, J. Wallauer, C. Winter, B. Huber, F. Endres and B. Roling, *Phys. Chem. Chem. Phys.*, 2012, **14**, 5090.
10 H. P. Steinrück, J. Libuda, P. Wasserscheid, T. Cremer, C. Kolbeck, M. Laurin, F. Maier, M. Sobota, P. S. Schulz and M. Stark, *Adv. Mater.*, 2011, **23**, 2571.
11 H. P. Steinrück, *Phys. Chem. Chem. Phys.*, 2012, **14**, 5010.
12 T. Waldmann, H.-H. Huang, H. E. Hoster, O. Höfft, F. Endres and R. J. Behm, *ChemPhysChem*, 2011, **12**, 2565.
13 B. Uhl, M. Roos, R. J. Behm, T. Cremer, F. Maier and H. P. Steinrück, *Phys. Chem. Chem. Phys.*, 2013, **15**, 17295.
14 F. Buchner, K. Forster-Tonigold, B. Uhl, D. Alwast, N. Wagner, A. Groß and R. J. Behm, *ACS Nano*, 2013, **7**, 7773.
15 B. Uhl, F. Buchner, D. Alwast, N. Wagner and R. J. Behm, *Beilstein J. Nanotechnol.*, 2013, **4**, 903.
16 L. Ruan, I. Stensgaard, F. Besenbacher and E. Laegsgaard, *Ultramicroscopy*, 1992, **42**, 498.
17 J. L. Domange and J. Oudar, *Surf. Sci.*, 1968, **11**, 124.

